ELSEVIER

Journal of Photochemistry and Photobiology A: Chemistry 133 (2000) 213–220

Journal of Photochemistry and Photobiology A:Chemistry

www.elsevier.nl/locate/jphotochem

Factors influencing relative efficiency in photo-oxidations of organic molecules by $Cs_3PW_{12}O_{40}$ and TiO_2 colloidal photocatalysts

Duane A. Friesen [a], Lara Morello [b], John V. Headley [a], Cooper H. Langford [b,*]

[a] *National Water Research Institute, Environment Canada, 11 Innovation Blvd., Saskatoon, SK, Canada S7N 3H5*

[b] *Department of Chemistry, The University of Calgary, 2500 University Drive NW, Calgary, AB, Canada T2N 1N4*

Received 3 November 1999; received in revised form 27 January 2000; accepted 7 February 2000

Abstract

This paper examines the factors influencing the efficiency of photo-oxidative degradation of *N*-methylpyrrolidinone (NMP) and atrazine by TiO_2 and $Cs_3PW_{12}O_{40}$ colloids, especially the roles of mechanism and substrate-photocatalyst interaction at the colloid surface. For both photocatalysts, major primary intermediates generated by the photo-oxidation of atrazine are the same. However, cyanuric acid appears to be oxidized by the UV irradiation of $PW_{12}O_{40}^{3-}$ in deaerated solution as evidenced by the formation of the heteropoly blue $PW_{12}O_{40}^{4-}$, suggesting that (in contrast to TiO_2) photo-oxidation is not solely due to hydroxyl radicals. Picosecond spectroscopy in water and simple alcohols indicates the importance of direct hydrogen abstraction by the excited tungstate. Quantum yields for the photo-oxidation of NMP by TiO_2 fit a Langmuir–Hinshelwood model, with a limiting quantum yield at high surface coverage of 0.029 ± 0.005 and an adsorption/desorption coefficient K of $2900\pm600\,M^{-1}$. For $Cs_3PW_{12}O_{40}$ under the same conditions, the quantum yield is 0.004–0.009 over the concentration range 10^{-5}–10^{-2} M. In the case of atrazine, an analogous treatment for $Cs_3PW_{12}O_{40}$ yields $K=1.4(\pm0.1)\times10^4$ M^{-1} while the value for TiO_2 is at least an order of magnitude less. The quantum yields indicate the importance of heterogeneity of the photocatalyst surface for $Cs_3PW_{12}O_{40}$, where the concentration dependence of the quantum yields can be explained by substrate adsorption at a small number of reaction sites, analogous to preassociation of dissolved polyoxotungstates and organic molecules.

Keywords: Photo-oxidation; Photocatalysis; Titanium dioxide; Polyoxometalate; Polyoxotungstate

1. Introduction

The application of photochemistry to environmental remediation and treatment of contaminated air and water is an active area of basic and applied research. One of the most widely studied schemes is the use of TiO_2 photocatalysis for the destruction of organic contaminants [1,2]. We now have a fair degree of understanding of some of the variables which pertain to TiO_2 photocatalysis (e.g. the generation and role of hydroxyl radical in aqueous TiO_2 slurries), although certain aspects (e.g. the role of substrate adsorption) continue to be matters for discussion. The limits to TiO_2 photocatalysis with respect to efficiency and range of contaminants degraded have encouraged efforts to address these issues by investigating other potential photocatalytic materials. One class of promising materials are polyoxotungstates, tungsten–oxygen clusters which are known to oxidize organic substrates upon UV irradiation [3–14]. Most photochemical studies have dealt with polyoxometalates in solution; however, recent investigations [15,16] have focused on the photocatalytic utility of desolubilized $Cs_3PW_{12}O_{40}$, an insoluble phosphotungstate catalyst previously known from thermal catalysis studies [17–19].

Recently, we have reported apparent mechanistic differences between TiO_2 and $Cs_3PW_{12}O_{40}$ in the photocatalytic degradation of a representative contaminant in water, *N*-methylpyrrolidinone (NMP) [16]. During the course of these studies, it became apparent that significant differences also exist in photo-oxidation efficiencies between the two photocatalysts. Observed efficiencies are dependent on several factors, including redox characteristics (ground- and excited-state), excited state lifetime (or in the case of TiO_2, the lifetime of the trapped hole-electron pair), and the roles of substrate adsorption and oxidation mechanism. In this paper, we examine the differences in photo-oxidation efficiencies for the destruction of two model substrates, NMP and atrazine (a triazine herbicide), upon UV irradiation of

* Corresponding author. Tel.: +1-403-220-3228; fax: +1-403-289-9488.
E-mail address: chlangfo@ucalgary.ca (C.H. Langford)

1010-6030/00/$ – see front matter
PII: S1010-6030(00)00237-9

TiO_2 and $Cs_3PW_{12}O_{40}$ to determine the role of excited state lifetime, photo-oxidation mechanism, and substrate adsorption.

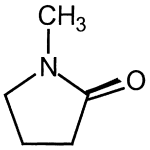

NMP

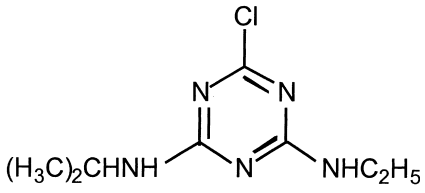

atrazine

2. Experimental

TiO_2 (P25 grade) was obtained from Degussa Corp. $H_3PW_{12}O_{40}$ was synthesized according to literature methods [20]. The UV absorption spectrum in acidic water was in agreement with literature spectra for $H_3PW_{12}O_{40}$ [3,13]. NMP was obtained from Aldrich. $Cs_3PW_{12}O_{40}$ was synthesized by the simple metathesis of concentrated solutions of CsCl and $H_3PW_{12}O_{40}$. The solid did not exhibit residual acidity. Atrazine was used as received from Supelco. 2-Propanol and 2-methyl-2-propanol (AnalaR) were used as received from BDH.

The picosecond transient absorption apparatus has been described in detail elsewhere [21]. Solutions of $H_3PW_{12}O_{40}$ were prepared with an absorbance of 0.5 in a 2 mm pathlength quartz cell. These were purged with argon for >10 min using a septum arrangement. Excitation was provided by the 355 nm third harmonic of a Nd-YAG laser (pulse width approximately 30 ps), with a pulse energy of 1.3–1.5 mJ. The spectra (between 425 and 675 nm) were an average of 10 individual measurements. Solutions were remixed between measurements.

Two arrangements were used for photocatalysis. The setup for NMP photocatalysis consisted of an annular quartz cell (volume 150 ml) which surrounded a 15 W lamp (Philips TUV low-pressure Hg lamp with output at 254 nm). Suspensions of the photocatalyst and aqueous contaminant solutions were kept aerated and stirred by a steady stream of air. The solutions were kept acidic (pH 3) with $HClO_4$. Incident light intensities were measured using ferrioxalate actinometry [22,23] and were determined to be $7.2(\pm 0.2)\times 10^{-6}$ einstein s^{-1}. A sufficiently concentrated actinometer solution ensured that approximately all of the light entering the cell was absorbed. Before the determination of quantum yield for NMP degradation, different photocatalyst loadings (between 0.25 and 2 g l^{-1}) were irradiated in the presence of dilute NMP to determine optimum levels for light absorption. For both photocatalysts, loading levels between 0.5 and 2 g l^{-1} resulted in the same rates of degradation within experimental error, signifying that at 0.5 g l^{-1} and above, the photocatalyst efficiently harvested 100% of the light entering the reactor. In comparison, the concentration of the substrate is low (consequently absorbance is low) in all experiments. The partition of light between the photocatalyst and the substrate is predominately to the photocatalyst.

The setup for atrazine photolysis utilized a front-face geometry and consisted of a medium-pressure Hg(Xe) arc lamp (200 W, Applied Photophysics) in conjunction with a 300 nm cutoff filter to eliminate shorter wavelength UV light. The cylindrical cell (volume=17.4 ml) was equipped with a flat quartz window which allowed passage of UV light. Solutions were kept thermostatted at 20–25°C.

Photocatalytic degradations were monitored using HPLC-UV (Waters 600E controller and 484 UV absorbance detector). For NMP, the degradation of NMP and formation of intermediates was monitored with isocratic elution (3–10% acetonitrile: 90–97% water, 1 ml min^{-1}) and a reversed-phase C_{18} NovaPak column. The detection wavelength was 212 nm. For atrazine, the same setup was used, with 63% water:37% acetonitrile elution and detection at 224 nm. Liquid chromatography–electrospray mass spectrometry (LC–MS) in the positive ion mode was performed at Agriculture and Agri-Food Canada (Calgary).

3. Results

3.1. Characteristics of photocatalyst material

$Cs_3PW_{12}O_{40}$ consists of 300 nm aggregates of small crystallites (10–12 nm diameter) with a BET surface area of $126\pm 8\ m^2\ g^{-1}$, a value consistent with observations of other workers as previously noted [16]. In comparison, the surface area of Dgussa TiO_2(P25) is $55\pm 1\ m^2\ g^{-1}$, in agrement with the manufacturer's literature. Previous studies have noted the insolubility of Cs-polyoxotungstate materials in water [17–19]. In highly basic solution, the colloidal polyoxometalate salt dissolved quickly and displayed a loss in the UV absorption spectrum above 230 nm, indicating a breakdown of the $PW_{12}O_{40}{}^{3-}$ unit [13]. At neutral or acidic pH values, the white colloid remained suspended in aqueous media; however, the small crystallite sizes precluded effective membrane filtration. Ultracentrifugation (30,000 rpm, 1 h) of acidic aqueous (pH 1–3) slurries of $Cs_3PW_{12}O_{40}$ resulted in solutions with a UV absorbance of <0.03 at 268 nm (1 cm cell), which corresponds to an apparent concentration of $<6\times 10^{-6}$ M for the dissolved fraction. (Note that even after ultracentrifugation, in some cases a minor amount of colloid appeared to be suspended in the solution.) Thus, the polyoxotungstate material is relatively insoluble in acidic solution.

3.2. Picosecond spectroscopy

The nature of the primary redox step in the photo-oxidation of alcohols by polyoxotungstates is still ambiguous [10]. To gain insight into the mechanism of the primary redox

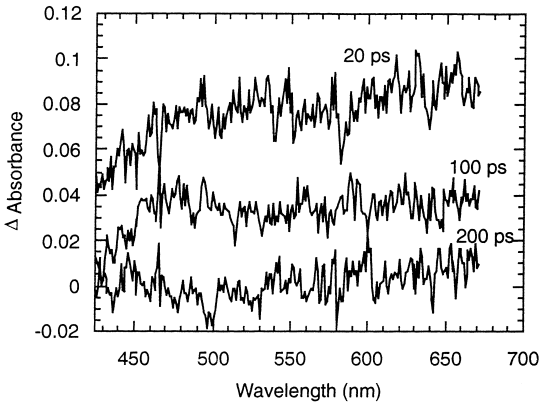

Fig. 1. Picosecond absorption spectra of a solution of $H_3PW_{12}O_{40}$ in water upon pulsed excitation at 355 nm.

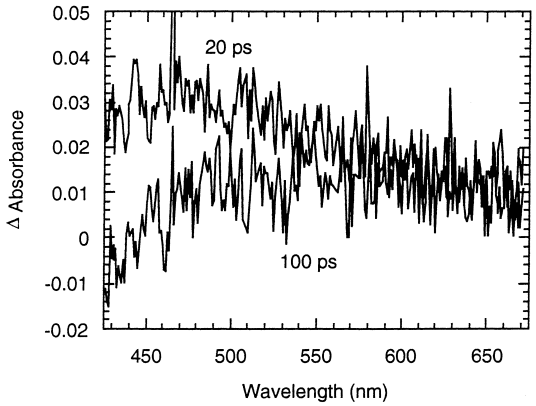

Fig. 3. Picosecond absorption spectra of a slurry of $Cs_3PW_{12}O_{40}$ in 2-propanol upon pulsed excitation at 355 nm.

event, picosecond spectra of dissolved $H_3PW_{12}O_{40}$ and $Cs_3PW_{12}O_{40}$ were obtained upon pulsed 355 nm excitation in 2-propanol, 2-methyl-2-propanol, and water. Solutions of $H_3PW_{12}O_{40}$ in water and 2-methyl-2-propanol show a broad, noisy (as is characteristic of this type of experiment), absorption feature (lifetime approximately 100 ps in both solvents) extending past 670 nm (Fig. 1). This band disappears within 200 ps and can be assigned to an LMCT excited state as observed previously for $PW_{12}O_{40}^{3-}$ in the unreactive solvent acetonitrile [9].

For $H_3PW_{12}O_{40}$ in 2-propanol, an initial transient with maximum absorbance between 450–500 nm appears within the laser pulse; then about 50 ps after the start of the pulse, absorption in the red region of the spectrum increases to produce a feature which persists on a much longer timescale (Fig. 2). This corresponds to the production of the 'heteropoly blue' $PW_{12}O_{40}^{4-}$ formed from one electron oxidation of the alcohol. It remains for seconds, as evidenced by a dark blue spot seen before remixing [3,4,9]. A similar sequence of events is observed for colloidal $Cs_3PW_{12}O_{40}$ at short timescales (Fig. 3). At longer timescales (>1 ns) an apparent absorption in the blue region becomes dominant for the colloid suspension. The nature of this absorption is unclear at this time, but it is similar to a feature observed for TiO_2 colloids. The most plausible assignment is that it may be due to a thermal lensing phenomenon.

3.3. Photodegradation of N-methylpyrrolidinone

Relative efficiencies of degradation were determined for the photo-oxidation of NMP by TiO_2 and $Cs_3PW_{12}O_{40}$. Quantum yields for heterogeneous systems are extremely difficult to measure due to light scattering by the colloidal materials, especially for front-face configurations [24–26]. In order to minimize the effect of scattered light, narrow-band irradiation (254 nm, a wavelength of high absorbance for both species) of both colloids in aqueous NMP solutions was performed with an annular quartz cell configuration, where the slurry completely surrounded the lamp. Photons are confined inside the configuration and are absorbed by the colloid particles, rather than being scattered to the outside (as occurs in a front-face configuration).

The concentration dependence of the relative quantum yield (ϕ) for NMP photodegradation in pH 3 solution is shown in Fig. 4. The extent of reaction was kept below 15–20% conversion. Measured quantum yields for the degra-

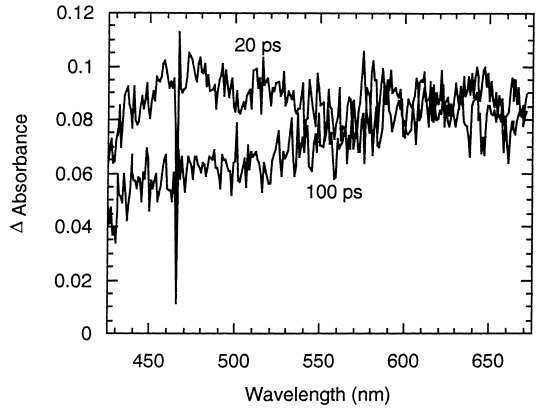

Fig. 2. Picosecond absorption spectra of a solution of $H_3PW_{12}O_{40}$ in 2-propanol upon pulsed excitation at 355 nm.

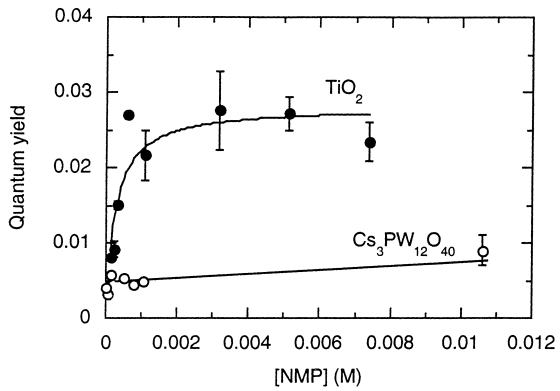

Fig. 4. Quantum yield versus NMP concentration at pH 3 for TiO_2 and $Cs_3PW_{12}O_{40}$ slurries (0.5 g l^{-1}, 254 nm irradiation).

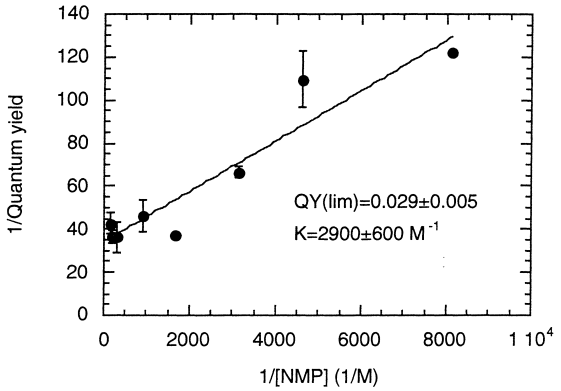

Fig. 5. Plot of reciprocal quantum yield versus reciprocal concentration for NMP photo-oxidation by TiO_2.

dation of NMP by TiO_2 appear to be approximately two to four times those for $Cs_3PW_{12}O_{40}$ at higher substrate concentrations (>0.5 mM). This is consistent with apparent relative efficiencies for the photocatalytic oxidation of 2-propanol by both photocatalysts [15]. However, the quantum yields at low NMP concentration (10^{-4} M) are comparable.

Langmuir–Hinshelwood (L–H) kinetics have been widely used for the interpretation of the rates of TiO_2 photocatalysis [1,27–30]. This model assumes an equilibrium of oxidizing and reducing species in a monolayer at the colloid surface. An equation can be derived on the basis of the L–H model which provides a value for the adsorption–desorption coefficient *K*, and for flim, the limiting quantum yield at high surface coverage [31]:

$$\frac{1}{\phi} = \frac{1}{\phi_{\lim}} + \frac{1}{\phi_{\lim} K[C_o]} \tag{1}$$

This equation is derived assuming greater adsorption by the substrate than by the reaction intermediates and products. For this reason, the quantum yields shown in Fig. 4 were measured at a low percent conversion of NMP. TiO_2 photocatalysis of NMP follows the typical pattern, with an apparent Langmuir–Hinshelwood dependence of quantum yield on concentration. When the data for TiO_2 are fitted to Eq. (1), a value for *K* of $2900 \pm 600\ M^{-1}$ is obtained (Fig. 5).

In the case of $Cs_3PW_{12}O_{40}$, the presence of only a small degree of curvature at low NMP concentration ($<10^{-4}$ M) indicates a very high *K* value, on the order of $10^5\ M^{-1}$. Dissolved polyoxotungstates such as $PW_{12}O_{40}^{3-}$ are known to show strong interactions with certain organics including NMP and chlorophenols; in fact, discrete polyoxotungstate–solvate complexes have been isolated and characterized [9]. These interactions are easily observed in solution by the appearance of absorption in the near-UV and visible regions of the spectrum due an intermolecular charge-transfer band of an electron donor–acceptor complex between solvent and polyoxotungstate [6,9,14,32]. For example, dissolved $PW_{12}O_{40}^{3-}$ forms a yellow–orange solution when mixed with aqueous phenol, and a light yellow solution when mixed with NMP.

Suspension of the white $Cs_3PW_{12}O_{40}$ colloid in NMP results in the formation of a light greenish color on the colloid. Similarly, the suspension of $Cs_3PW_{12}O_{40}$ in an aqueous phenol solution results in the formation of a yellow–orange colored colloid. These results indicate that the organic species can interact with the insoluble polyoxometalate on the surface of the colloid, analogous to the complexation between organics and dissolved $PW_{12}O_{40}^{3-}$. (The colour is not of known origin although a CT process seems most likely. However, diagnosis of interaction is unmistakable.) As the water content is increased the interaction is lessened as evidenced by a loss of color on the colloid. These results suggest that preadsorption may therefore play an important role in the photo-oxidation of NMP by $Cs_3PW_{12}O_{40}$.

To examine the role of adsorption in the absence of UV irradiation, slurries of $10\ g\ l^{-1}$ $Cs_3PW_{12}O_{40}$ or TiO_2 were shaken overnight in the presence of 10 and 100 ppm NMP. It was found that the concentration of dissolved NMP remained constant within the experimental detection limits (<2% difference). Approximate upper limits for the number of adsorbing sites were estimated by fitting the limits for equilibrium concentration (C_{eq}) to Eq. (2) [28], with the assumption that binding constants (*K*) are the same for photocatalysis and dark adsorption.

$$n = \frac{n_{\max} K C_{\text{eq}}}{1 + K C_{\text{eq}}} \tag{2}$$

In this equation, *n* represents the number of moles adsorbed and $n_{\max}$ the maximum number of sites. Based on a *K* value of $2900\ M^{-1}$ for NMP on TiO_2 and a determined limit of 2% as the smallest concentration change that can be detected reliably for the HPLC analysis, the maximum number of sites ($n_{\max}$) is $1\times10^{-6}\ mol\ g^{-1}$. A similar analysis for $Cs_3PW_{12}O_{40}$ yields an upper limit of $2.5\times10^{-7}\ mol\ g^{-1}$. In comparison, corresponding values for monolayer adsorption of aromatic substrates on TiO_2 range from $7\times10^{-5}\ mol\ g^{-1}$ for salicylic acid at natural pH to approximately $1–2\times10^{-6}\ mol\ g^{-1}$ for the isomers of chlorophenol [28]. These results indicate that, compared to TiO_2, photocatalysis of NMP by $Cs_3PW_{12}O_{40}$ involves stronger interaction at a smaller number of sites on the colloid surface.

3.4. Photocatalytic degradation of atrazine

The degradation of atrazine by direct photolysis and by TiO_2 photocatalysis is well-known and many of the intermediates have been identified [33–37]. Because of the complication of extensive direct photolysis by 254 nm light, the output of a 200 W Xe(Hg) arc lamp with cutoff filter (>300 nm irradiation) was used as the irradiation source. Since not all of the photons were absorbed by the photocatalyst due to the polychromatic nature of the irradiation, the resulting quantum yield values only represent a lower limit and are denoted by ϕ' in the subsequent discussion. For the determination

of intermediates, a solution of 33 ppm atrazine was irradiated in the presence of 2 g l^{-1} TiO_2 for 10 min or 2 g l^{-1} $Cs_3PW_{12}O_{40}$ for 30 min. Different irradiation times were used because of the difference in degradation efficiencies for the two photocatalysts (see below). Major intermediates detected by LC–MS in the present study are shown below.

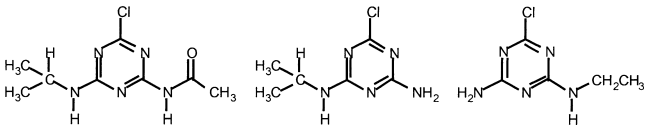

1 CIAT CEAT

These are observed at early timescales for both TiO_2 and $Cs_3PW_{12}O_{40}$ photo-oxidation. As expected, the photocatalytic activity is centred on the alkylamine side-chains. Compound 1 and CIAT arise from oxidative attack on the ethylamine substituent, whereas CEAT is derived from attack on the isopropylamine substituent. In the case of TiO_2, it known that the final product of photodegradation is cyanuric acid, which is resistant to hydroxyl radical attack [33,36]. In contrast, when cyanuric acid is irradiated under anaerobic conditions in the presence of dissolved $H_3PW_{12}O_{40}$, the characteristic 'heteropoly blue' arising from $PW_{12}O_{40}{}^{4-}$ is observed, indicating oxidation of the organic substrate.

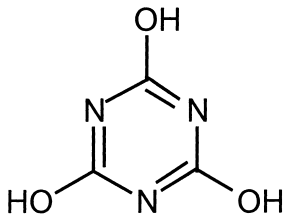

cyanuric acid

Photo-oxidation of cyanuric acid by the heterogeneous $Cs_3PW_{12}O_{40}$ gave inconclusive results, since it appeared that measurable amounts of the cyanuric acid were adsorbed onto the photocatalyst under both the presence and absence of UV irradiation. This may have hindered efficient photoreaction due to lack of product desorption.

The concentration dependence of the apparent photo-oxidation efficiency for atrazine degradation by TiO_2 and $Cs_3PW_{12}O_{40}$ shows similarities to that for NMP. The apparent quantum yield for $Cs_3PW_{12}O_{40}$ has a curved dependence on atrazine concentration between 0–250 mM (Fig. 6). A linear plot is obtained from a graph of ϕ'^{-1} versus $[\text{atrazine}]^{-1}$, with a derived K value of $1.4(\pm0.1)\times104\,M^{-1}$. For TiO_2, an almost linear dependence is observed up to 50 ppm (230 mM), near the limit of solubility of atrazine in water. This precluded a precise determination of K, but it is on the order of 10^3 or less for TiO_2. It is assumed that the curvature would occur at higher substrate concentration if not precluded by solubility factors, as is observed for NMP and other organic compounds [28,31]. These results are again supportive of a higher degree of adsorption for $Cs_3PW_{12}O_{40}$.

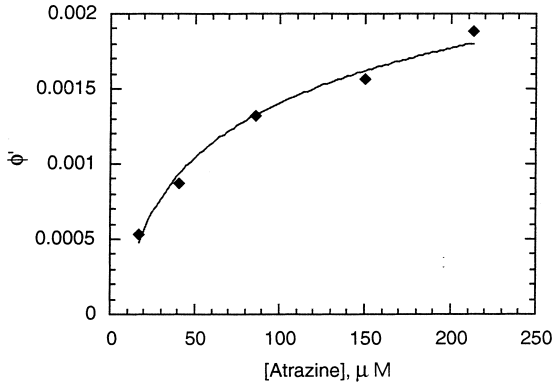

Fig. 6. Apparent quantum yield ϕ' versus concentration of atrazine for $Cs_3PW_{12}O_{40}$ slurries (2 g l^{-1}). L–H parameters derived from plot (see text for details): $K=1.4(\pm0.1)\times10^4\,M^{-1}$; ϕ' ('apparent quantum yield')$=2.3(\pm0.1)\times10^{-3}$.

4. Discussion

4.1. Picosecond spectroscopy

It is generally accepted that in aqueous suspension, the primary photocatalytic pathway for TiO_2 is the oxidation of adsorbed water to form hydroxyl radicals [1,24,25]. It is these radicals which initiate the oxidation of organic contaminants, although the direct oxidation of adsorbed organics on the TiO_2 surface is also possible at high concentration [25]. With polyoxotungstates, the picture is not as clear. Photo-oxidation of organics by dissolved polyoxotungstates may proceed via direct electron transfer or by hydrogen abstraction by either the excited polyoxometalate or a generated hydroxyl radical [3,10,11]. Picosecond absorption spectroscopy allows a view of the primary photoinduced events following excitation of dissolved $PW_{12}O_{40}{}^{3-}$ and colloidal $Cs_3PW_{12}O_{40}$.

Oxidation of 2-propanol by both dissolved photo-excited $PW_{12}O_{40}{}^{3-}$ and $Cs_3PW_{12}O_{40}$ colloid proceeds through an initial transient with an absorbance maximum in the blue region, and a long-lived product with the characteristic $PW_{12}O_{40}{}^{4-}$ spectrum. Conversely, 2-methyl-2-propanol shows an LMCT absorption which decays to baseline within 200 ps. This appears to disfavor direct electron transfer as the primary photochemical step. The electrochemical oxidation potentials for both alcohols are similar [38], therefore, implying that the prompt redox behavior should also be similar if direct electron transfer was the initial step. (The excited potential of POM is estimated at 2.63 V versus NHE (38), the two alcohols have potentials of 2.5–2.6 V. Direct electron transfer is only possible if it can proceed without a significant overpotential.) It appears that the presence of a hydrogen atom on the carbon bound to the hydroxyl group is critical. Many studies have established the ability of polyoxometalates to functionalize hydrocarbons by H-abstraction [10].

The observation of an initial transient formed before the final reduced $PW_{12}O_{40}{}^{4-}$ appears is similar to the photo-

redox behavior for $PW_{12}O_{40}^{3-}$ in neat NMP [32]. Alcohols are believed to weakly associate with polyoxotungstates [5,39], and in analogy to the NMP case, the initial transient may represent the excited state of the weak association [32]. Relaxation, possibly by hydrogen transfer from the α-carbon of 2-propanol, would result in the formation of the characteristic long-lived $PW_{12}O_{40}^{4-}$ spectrum.

The data for neat alcohol solutions does not allow a conclusive decision between direct H-abstraction by the excited polyoxometalate and H-abstraction by a photogenerated hydroxyl radical for aqueous phase $PW_{12}O_{40}^{3-}$ photo-oxidations. However, product distributions for $Cs_3PW_{12}O_{40}$ photo-oxidations of aqueous solutions of NMP suggest that both mechanisms may occur [16]. It is notable that the behavior of excited $PW_{12}O_{40}^{3-}$ in water and 2-methyl-2-propanol on picosecond timescales is the same. This suggests that large-scale generation of long-lived OH radicals in water (with corresponding reduction of the tungstate to $PW_{12}O_{40}^{4-}$) may be unlikely. While this does not eliminate the possibility of OH radicals on the colloid surface at short timescales, it is unlikely that OH-promoted oxidations comprise the only reaction pathway.

4.2. Photogenerated intermediates

The primary intermediates generated from atrazine by both photocatalysts are the result of oxidation processes. However, the overall oxidation may occur through different mechanistic pathways as shown previously for NMP [16]. It has been shown that cyanuric acid is relatively impervious to hydroxyl radical attack and is therefore, the final product resulting from the TiO_2-photocatalyzed oxidation of atrazine [34]. In contrast, the generation of the heteropoly-blue $PW_{12}O_{40}^{4-}$ in irradiated N_2-saturated solutions of $H_3PW_{12}O_{40}$ and cyanuric acid indicates that the excited polyoxotungstate can oxidize cyanuric acid. This implies that there are mechanistic pathways other than hydroxyl radical formation for polyoxometalate oxidations. The ability of polyoxometalates to undergo two-electron reduction and to directly abstract a H-atom from a substrate opens new pathways for photo-oxidative degradation. In fact, it has been shown that polyoxometalates continue to function as photo-oxidative agents under anaerobic conditions which severely retard TiO_2 photocatalysis [40]. In this context, it is interesting to note that recent studies indicated that atrazine can be mineralized by a mixed TiO_2-alkylvanadate photocatalyst [41]. One may note, however, that contributions from a parallel pathway involving generated hydroxyl radicals are not ruled out, as is suggested by similarities in the intermediates generated for NMP photo-oxidation by TiO_2 and $Cs_3PW_{12}O_{40}$ [16].

4.3. Photocatalytic efficiencies

As has been shown previously, redox potentials for NMP oxidation are favorable for both photocatalysts [16]. Our results show that the lifetime of the excited LMCT state of $PW_{12}O_{40}^{3-}$ is around 100 ps in water. In contrast, trapped electron-hole pairs for TiO_2 can possess lifetimes of 10–100 ns [1]. In the absence of other effects (e.g. differences in adsorption characteristics) the difference in lifetimes alone would imply a lower oxidation efficiency for polyoxotungstate as compared to TiO_2.

However, the concentration dependence of the quantum yields for NMP degradation by TiO_2 and $Cs_3PW_{12}O_{40}$ suggests a much deeper level of complexity. In particular, Fig. 4 shows that TiO_2 clearly possesses a higher efficiency for photo-oxidation at NMP concentrations higher than 0.5 mM. At concentrations much lower than this the quantum yields for TiO_2 and $Cs_3PW_{12}O_{40}$ are similar. Furthermore, the quantum yield for $Cs_3PW_{12}O_{40}$ oxidation of NMP is nearly invariant over a concentration range of three orders of magnitude (10^{-5}–10^{-2} M). These findings suggest that reactions of molecules adsorbed at the colloid/solution interface may be important.

Adsorption appears to play a key role in semiconductor photocatalyst chemistry. Xu and Langford have shown that support of TiO_2 on an adsorptive ZSM-5 zeolite can increase the relative photocatalytic degradation activity of acetophenone in water [42]. Hoffmann et al. have shown that pH markedly influences the rate of photocatalysis of various organic acids and amines, with degradation highly reduced at pH values corresponding to conditions which discourage binding of the ionized substrate to the TiO_2 surface [43].

The value for K from the L–H treatment of TiO_2-promoted NMP oxidation is comparable to values for chlorophenol and other compounds [1,28]. However, the observed lack of dark adsorption places limits on the number of effective adsorption sites. This may be manifested in the relatively low limiting quantum yield (<0.03) for NMP oxidation by TiO_2. Photons may be wasted on unproductive sites, i.e. sites where charge recombination between hydroxyl radicals and electrons occurs more quickly than reaction with a non-adsorbed NMP molecule. It is interesting to note that Bolton et al. have determined a quantum yield of 0.04 for TiO_2-promoted oxidation of 0.03 M methanol, another substrate expected to be a relatively poor adsorber in aqueous solution [25].

The picture with $Cs_3PW_{12}O_{40}$ is more extreme. The near-constancy of ϕ over the range 10^{-5}–10^{-2} M implies a higher K value, while the low amount of dark adsorption indicates a very small number of adsorption sites. Evidence from two sources backs this interpretation.

The first argument takes into account the kinetic data. The following scheme can be used to estimate a reaction rate for the oxidation of NMP (and reduction of $PW_{12}O_{40}^{3-}$) [3]:

$$PW_{12}O_{40}^{3-} \xrightarrow{I_a} {}^{\bullet}PW_{12}O_{40}^{3-},$$

$$I_a = 4.8 \times 10^{-5}\ \text{einstein}\ l^{-1}\ s^{-1}$$

$${}^{\bullet}PW_{12}O_{40}^{3-} \xrightarrow{k_1} PW_{12}O_{40}^{3-}, \quad k_1 = 10^{10}\ s^{-1}$$

$$\mathrm{NMP} + {}^{\bullet}\mathrm{PW_{12}O_{40}}^{3-} \xrightarrow{k_2} \mathrm{PW_{12}O_{40}}^{4-} + \mathrm{NMP}^{+}, \quad k_2$$

$$\text{Rate of } \mathrm{PW_{12}O_{40}}^{4-} \text{ formation} = \frac{k_2 \times [\mathrm{NMP}] \times I_a}{k_1 + k_2 \times [\mathrm{NMP}]}$$

At a concentration of 10^{-5} M NMP (1 ppm), the quantum yield for destruction of NMP by $Cs_3PW_{12}O_{40}$ is still 0.004, indicating that the rate of NMP oxidation is $1.9\times10^{-7}\,\mathrm{M\,s^{-1}}$ and the rate of $\mathrm{PW_{12}O_{40}}^{4-}$ production is $3.8\times10^{-7}\,\mathrm{M\,s^{-1}}$ (since the overall oxidation of NMP is a two electron process). The resulting value for k_2 is $8\times10^{12}\,\mathrm{M^{-1}\,s^{-1}}$; this is several orders of magnitude above the diffusion-controlled limit of $10^{10}\,\mathrm{M^{-1}\,s^{-1}}$ [14]. This suggests preassociation of NMP at the colloid surface. These calculations are complicated by the fact that the polyoxometalate is a heterogeneous colloid rather than a dissolved species. However, the magnitude of the calculated rate constant and the small size of the colloid still suggest that this treatment is qualitatively valid.

The presence of surface interaction is also evidenced by the development of a color change for $Cs_3PW_{12}O_{40}$ in the presence of NMP or phenol. These parallel the development of a colored solution for mixtures of $H_3PW_{12}O_{40}$ and NMP or aqueous phenol which is due to the formation of a molecular association [6,9,14,32]. Einaga and Misono demonstrated complexation between 4-chlorophenol and $H_3PW_{12}O_{40}$ by the development of an absorption band in the visible region [14]. They also found that the rate constant for the photo-oxidation of 4-chlorophenol by dissolved $\mathrm{PW_{12}O_{40}}^{3-}$ was greater than the diffusion-controlled limit, suggesting preassociation. Studies by Fox et al. [5] and Hill et al. [39] also suggest organic molecule-polyoxometalate interaction.

Considering the measurable degradation rates and low degree of surface adsorption, this behavior may be indicative of strong binding at a small number of sites. Heterogeneity of sites may thus play an important role for both photocatalysts [44]. Xu and Langford have recently found that the adsorption isotherm of acetophenone onto TiO_2 in aqueous solution shows evidence of a small number of strongly adsorbing sites (typical Langmuir isotherm at low concentration) and a higher density of weakly-adsorbing sites (linear increase in amount of adsorbed acetophenone at higher concentration) [45]. The Langmuir–Hinshelwood parameters from the photo-oxidation of acetophenone follow those derived from dark adsorption, suggesting that it may be the relatively low number of strongly interacting sites which are responsible for the bulk of the photo-oxidation.

The efficiencies for atrazine photo-oxidation appear to follow those for NMP, i.e. the apparent binding constant K for $Cs_3PW_{12}O_{40}$ exceeds that of TiO_2. These results suggest that surface interaction of organic molecules with $Cs_3PW_{12}O_{40}$ analogous to molecular association with $\mathrm{PW_{12}O_{40}}^{3-}$ in solution may be a general phenomenon; however, quantum yields may stay low because of the low density of effective adsorption or reaction sites.

5. Conclusions

TiO_2 and $Cs_3PW_{12}O_{40}$ both show photocatalytic activity towards the oxidation of NMP and atrazine. However, the two materials show differences in terms of concentration dependence of the quantum yields for photo-oxidation. It appears that, in the case of the polyoxotungstate, surface interactions between photocatalyst and substrate are important. This is reflected in substantially higher K values derived from a Langmuir–Hinshelwood model for the $Cs_3PW_{12}O_{40}$ photo-oxidation of both NMP and atrazine.

Acknowledgements

The authors wish to thank the Natural Sciences and Engineering Research Council of Canada for financial support, Ms. Vivian Sun for technical assistance, the Plant Biotechnology Institute of the National Research Council (Dr. E. Tsang) for autosampler HPLC analysis, and Agriculture and Agri-Food Canada (Calgary) for LC-MS analysis. The picosecond experiments were performed at the Canadian Centre for Picosecond Laser Spectroscopy at Concordia University, Montreal with the assistance of Mr. R. Danesh.

References

[1] M.R. Hoffman, S.T. Martin, W. Choi, D.W. Bahnemann, Chem. Rev. 95 (1995) 69.
[2] D.F. Ollis, H. Al-Ekabi (Eds.), Photocatalytic Purification and Treatment of Water and Air, Elsevier, Amsterdam, 1993.
[3] E. Papaconstantinou, Chem. Soc. Rev. 18 (1989) 1.
[4] D. Dimotikali, E. Papaconstantinou, Inorg. Chim. Acta 87 (1984) 177.
[5] M.A. Fox, R. Cardona, E. Gaillard, J. Am. Chem. Soc. 109 (1987) 6347.
[6] C.L. Hill, D.A. Bouchard, J. Am. Chem. Soc. 107 (1985) 5148.
[7] R.F. Renneke, M. Kadkhodayan, M. Pasquali, C.L. Hill, J. Am. Chem. Soc. 113 (1991) 8357.
[8] T. Yamase, T. Usami, J. Chem. Soc., Dalton Trans. (1988) 183.
[9] C.L. Hill, D.A. Bouchard, M. Kadkhodayan, M.M. Williamson, J.A. Schmidt, E.F. Hilinski, J. Am. Chem. Soc. 110 (1988) 5471.
[10] C.L. Hill, C.M. Prosser-McCartha, in: K. Kalyanasundaram, M. Grätzel (Eds.), Photosensitization and Photocatalysis Using Inorganic and Organometallic Compounds, Kluwer, Dordrecht, 1993, pp. 307–330.
[11] A. Mylonas, E. Papaconstantinou, J. Photochem. Photobiol. A. 94 (1996) 77.
[12] A. Mylonas, A. Hiskia, E. Papaconstantinou, J. Mol. Catal. A. 114 (1996) 191.
[13] H. Einaga, M. Misono, Bull. Chem. Soc. Jpn. 69 (1996) 3435.
[14] H. Einaga, M. Misono, Bull. Chem. Soc. Jpn. 70 (1997) 1551.
[15] D.A. Friesen, D.B. Gibson, C.H. Langford, J. Chem. Soc., Chem. Commun. (1998) 543.
[16] D.A. Friesen, J.V. Headley, C.H. Langford, Environ. Sci. Technol. 33 (1999) 3193.
[17] Y. Izumi, M. Ono, M. Kitagawa, M. Yoshida, K. Urabe, Microporous Mater. 5 (1995) 255.
[18] Y. Izumi, M. Ono, M. Ogawa, K. Urabe, Chem. Lett. (1993) 825.
[19] T. Okuhara, N. Mizuno, M. Misono, Adv. Catal. 41 (1996) 113.
[20] H. Wu, J. Biol. Chem. 43 (1920) 189.

[21] L. Persaud, Ph.D. Thesis, Concordia University, Montreal, Canada, 1985.
[22] C.G. Hatchard, C.A. Parker, Proc. R. Soc. A 235 (1956) 518.
[23] A.D. Kirk, C. Namasivayam, Anal. Chem. 55 (1983) 2428.
[24] N. Serpone, J. Photochem. Photobiol. A 104 (1997) 1.
[25] L. Sun, J.R. Bolton, J. Phys. Chem. 100 (1996) 4127.
[26] C.A. Martin, M.A. Baltanas, A.E. Cassano, J. Photochem. Photobiol. A 94 (1996) 173.
[27] J. Cunningham, P. Sedlak, J. Photochem. Photobiol. A 77 (1994) 255.
[28] J. Cunningham, P. Sedlak, in: D.F. Ollis, H. Al-Ekabi (Eds.), Photocatalytic Purification and Treatment of Water and Air, Elsevier, Amsterdam, 1993, pp. 67–82.
[29] A. Mills, S. Morris, J. Photochem. Photobiol. A 71 (1993) 75.
[30] J. Cunningham, G. Al-Sayyed, J. Chem. Soc., Faraday Trans. 86 (1990) 3935.
[31] G.P. Lepore, B.C. Pant, C.H. Langford, Can. J. Chem. 71 (1993) 2051.
[32] J.A. Schmidt, E.F. Hilinski, D.A. Bouchard, C.L. Hill, Chem. Phys. Lett. 138 (1987) 346.
[33] K.C. Pugh, D.J. Kiserow, J.M. Sullivan, J.H. Grinstead, Jr., in: Emerging Technologies in Hazardous Waste Management V, ACS, Washington, 1995, pp. 174–194.
[34] E. Pelizzetti, V. Maurino, C. Minero, V. Carlin, E. Pramauro, O. Zerbinati, M.L. Tosato, Environ. Sci. Technol. 24 (1990) 1559.
[35] G.K.C. Low, S.R. McEvoy, R.W. Matthews, Environ. Sci. Technol. 25 (1991) 460.
[36] P.L. Yue, D. Allen, in: D.F. Ollis, H. Al-Ekabi (Eds.), Photocatalytic Purification and Treatment of Water and Air, Elsevier, Amsterdam, 1993, pp. 607–612.
[37] A. Torrents, B.G. Anderson, S. Bilboulian, W.E. Johnson, C.J. Hapeman, Environ. Sci. Technol. 31 (1997) 1476.
[38] V.D. Parker, G. Sundholm, U. Svanholm, A. Ronlan, O. Hammerich, in: Encyclopedia of Electrochemistry of the Elements, Vol. 11, Marcel Dekker, New York, 1978, Ch XI-2.
[39] C.L. Hill, R.F. Rennecke, L. Combs, Tetrahedron 44 (1988) 7499.
[40] R.C. Chambers, C.L. Hill, Inorg. Chem. 30 (1991) 2776.
[41] I.R. Bellobono, P.L. Pinacci, G. Riva, C. Lagrasta, Fresenius Environ. Bull. 7 (1998) 277.
[42] Y. Xu, C.H. Langford, J. Phys. Chem. 99 (1995) 11501.
[43] C. Kormann, D.W. Bahnemann, M.R. Hoffmann, Environ. Sci. Technol. 25 (1991) 494.
[44] P. Sawunyama, A. Fujishima, K. Hashimoto, J. Chem. Soc. Chem. Commun. (1998) 2229.
[45] Y. Xu, C.H. Langford, in preparation.